

Determination of thermal and elastic coefficients of optical thin-film materials

S. Michel*, F. Lemarquis and M. Lequime

Institut FRESNEL – UMR CNRS 6133
Domaine Universitaire de Saint-Jérôme, 13397 Marseille Cedex 20 – France

ABSTRACT

In the aim of describing the thermo-mechanical behaviour of a thin-film filter, simplified models have been studied. An easy way is to determine the evolution of the optical properties of each layer composing the stack, and thus to derive the features change at the component level. Therefore, the knowledge of physical parameters describing each material, such as the coefficient of thermal expansion, the thermo-optic coefficient, the Poisson's ratio and the elasto-optic coefficients, is required. The main challenge is to evaluate these parameters at a single layer level. We propose here a new optical method, based on the analysis of the thermal behaviour of two dedicated Fabry-Perot (FP) structures including a thin disk of the material under study. In parallel, we show through modelling, that we can determine the physical properties of this material with a high accuracy, only by measuring the shift of FP resonance wavelengths. However, we have to take into account the mechanical deformation of the Fabry-Perot structures induced by the thin-film deposition process as well as its evolution with the temperature change (thermal stresses). In this goal, we carried out an accurate study of the thermo-mechanical behaviour of our interferometric structures by using a Finite Element Method.

Keywords: Thin-film, coefficient of thermal expansion, Poisson ratio, thermal stress.

Corresponding authors: sebastien.michel@fresnel.fr

1. INTRODUCTION

The environmental behavior of thin-film coatings, especially the evolution of their optical properties under thermal or mechanical stresses, is a key feature for a lot of demanding applications. As an example, the thermal stability of the central wavelength of narrow-bandpass filters needs to be better than $1\text{pm}/^\circ\text{C}$ to cope with the stringent requirements of Dense Wavelength Division Multiplexing (DWDM) telecommunications networks.

Until now, this subject has been studied with simplified models to take into account the mechanical and thermal properties of both the coating and the substrate. The model developed by Takashashi [1] in 1995 considers the whole coating as a single equivalent layer that interacts with the substrate. This model was applied with a great success to the stabilization of the centering wavelength of narrow-bandpass filters versus temperature changes by selecting a substrate with an appropriate Coefficient of Thermal Expansion (CTE), about $110.10^{-7}(\text{C})^{-1}$. However, the thermal and mechanical properties attributed to this single equivalent layer are quite difficult to identify and most of the time, the properties of the bulk material corresponding to the spacer are used. Our team has proposed in 2003 an alternative model [2,3] which leads to the same conclusions that the Takashashi's one, but which requires the knowledge of a lot of physical parameters describing the mechanical behavior of the same single equivalent layer, i.e. its coefficient of thermal expansion α , its thermo-optic coefficient β , its Poisson's ratio ν and its photo-elastic coefficients p_{11} and p_{12} . Thereafter, the problem of the description of this single equivalent layer remains complete, but this new model can be easily upgraded to the analysis of a stack, which requires this time the knowledge of the same physical coefficients, but for each elementary layer.

The main difficulty to determine these parameters comes from the fact that, for single layers, the evolution of the optical properties remains always very small and depends on the deposition process. To illustrate this issue, we give the example of the CTE of tantala thin films, which have been evaluated to the following values by different methods and deposition processes: $\alpha_L = -4.4.10^{-5}/^\circ\text{C}$ [4], $\alpha_L = 0.2.10^{-5}/^\circ\text{C}$ [5] and $\alpha_L = 0.6.10^{-5}/^\circ\text{C}$ [6].

As a consequence, it has been required to develop a specific and very accurate measurement method. This method is an interferometric one and involves the use of dedicated Fabry-Perot structures. To assess the optical behavior of our interferometric structures, we developed a complete simulation software to first calculate the evolution of the optical properties of single layer structures under thermal or mechanical stresses, and then to determine the data processing able to recover, from only optical measurements, the different coefficients used in calculations.

Nevertheless, this optical approach is not sufficient to hope measuring with a high precision the coefficients of thin films. Indeed, applying a thermal change on a structure with different materials causes its deformation by curving the interferometer blades. To precisely evaluate this deformation, we carried out an accurate study on the thermo-mechanical behavior of our Fabry-Perot interferometers by using a Finite Element Method. Finally, we obtain canonical structures dedicated to the extraction of the thermal and elastic properties of thin films.

2. FIRST APPROACH

As we said in introduction, we aim to evaluate the coefficients describing the evolution of thickness and refractive index for thin films involved in a stack. This implies to study the behavior of each layer deposited alone on a substrate. Moreover, to evaluate the substrate effect, it is necessary to consider a differential configuration with two regions, one with the layer, and the other without it, as represented in Fig. 1.

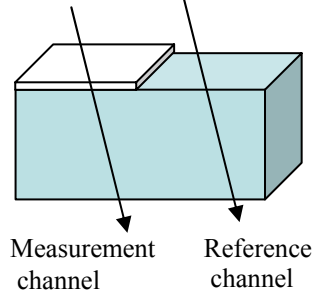


Figure 1: Differential configuration envisaged to precisely evaluate the behavior of one layer under mechanical or thermal stress

First, we consider that the thickness and refractive index variations under a thermal change are given by the common relations $\frac{\Delta t_L}{t_L} = \alpha_L \Delta T$ and $\frac{\Delta n_L}{n_L} = \beta_L \Delta T$. For a silica layer having the same properties than a fused silica glass, we

obtain for a 1 μm thick layer and a thermal change $\Delta T=50^\circ\text{C}$, an absolute variation of thickness equal to 50 pm, and an absolute variation for refractive index equal to $5 \cdot 10^{-4}$. The common technique to evaluate the thickness and the refractive index of a layer is to measure the transmittance and the reflectance spectrum versus the wavelength λ . The typical accuracy obtained on each term is respectively 1 nm and 10^{-2} . However, it is not adapted to our problem as we want to detect variations one hundred times less than the cited ones. It is therefore necessary to enhance the sensitivity of the measurements. Moreover, we aim to separate the effects of thickness variations from the refractive index ones, in order to measure the coefficients associated to each of them. A well-known method is to use a Fabry-Perot cavity to enhance the effects by detecting the wavelengths shifts on the transmittance spectrum of the interferometer. Nevertheless, the sensitivity of the measurement is in relation with the finesse of the Fabry-Perot, and thus to increase it, we consider silver coatings to have a good reflectance for the mirrors composing the interferometer. We envisaged two Fabry-Perot structures, represented in Fig. 2 and Fig. 3. Each of them possesses one reference and one measurement channel, this latter being distinguished from the first one by the fact that there is an additional dielectric layer we want to study. The basic idea is to compare the behavior (by the intermediate of wavelengths shifts) between the two channels under a thermal change, and to extract the only part due to the dielectric layer. The cavity of the Fabry-Perot is composed by the air layer separating the two mirrors.

For the first structure (Fig. 2), called thermo-mechanical configuration, the dielectric layer to investigate is deposited in the shape of a circular disk at the centre of the two substrates which compose the interferometer. This process can be made by a masking operation. A silver coating is then deposited on the whole of structures to form the mirrors. As the Fabry-Perot effect gives information mainly between the two mirrors, i.e. the two silver coatings, this structure is mainly sensitive to the thickness variations of the dielectric layer.

For the second structure (Fig. 3), called thermo-optical configuration, the dielectric layer to characterize is deposited inside the cavity, above the silver coatings. These structures will be sensitive to the optical thickness variation under the temperature change. To isolate in this result the contribution of the refractive index variation, we need to take into account the result on the thickness variation established with the first structure.

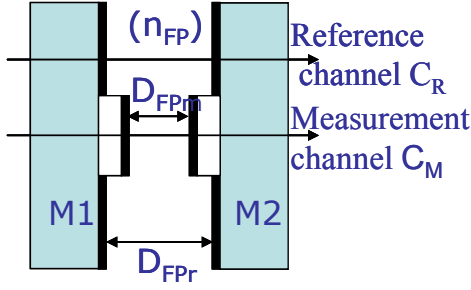


Figure 2: Thermo-mechanical Fabry-Perot configuration. The dielectric layer to study is below the silver thin film

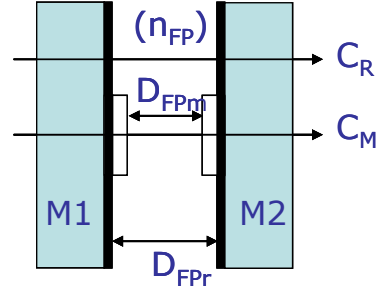


Figure 3: Thermo-optical Fabry-Perot configuration. The dielectric layer is inside the cavity, above the silver thin film.

As we describe in Section 3, the first structure gives access to the CTE α_L and the Poisson's ratio ν_L of the dielectric layer (under a thermal change ΔT) and the study of the second structure determine the temperature coefficient of refractive index (TCRI) β and the elasto-optics coefficients p_{11} and p_{12} . In this paper, we report only on our theoretical results obtained on the thermo-mechanical configuration.

3. PRINCIPLE OF MEASUREMENT OF α_L AND ν_L

Considering a single layer (thickness t_L , refractive index n_L) deposited on a substrate, as represented in Fig. 4. The layer (respectively the substrate) is described by its CTE α_L (resp. α_S) and its Poisson ratio ν_L . Under a thermal change ΔT , the thickness and refractive index variations are given by [3]:

$$\frac{1}{\Delta T} \frac{\Delta t_L}{t_L} = \alpha_L - \frac{2\nu_L}{1-\nu_L} (\alpha_S - \alpha_L) = A\alpha_S + B \quad (1)$$

$$\frac{1}{\Delta T} \frac{\Delta n_L}{n_L} = \beta_L - \frac{n_L^2}{2} [(1-\nu_L)p_{11} + (1-3\nu_L)p_{12}] \frac{(\alpha_S - \alpha_L)}{1-\nu_L}. \quad (2)$$

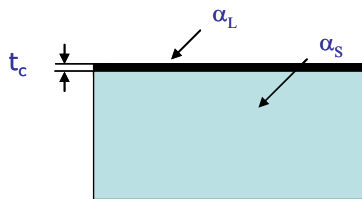


Figure 4: Single dielectric layer deposited on a substrate. This structure allows us to study the optical thickness variation under a thermal change.

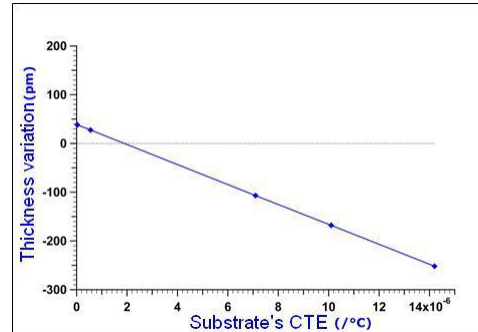


Figure 5: Thickness variation for a silica layer versus the CTE of the substrate. The thermal change ΔT is 50°C .

Eq. 1 shows a linear dependence of the quantity Δt_L versus the CTE of the substrate α_S . Therefore, considering several substrates with different CTE, the slope of the straight line $\Delta t_L=f(\alpha_S)$ allows us to evaluate the Poisson ratio of the dielectric layer while its crossing with the $\alpha_S=0$ axis give access to the CTE). Figure 5 illustrates the relationship $\Delta t_L=f(\alpha_S)$ for a silica layer described by the same properties than the bulk material. According to Eq. 1 notations, we can express the slope and the specific value at $\alpha_S=0$, as follows:

$$\nu_L = \frac{A}{A-2}, \alpha_L = B \frac{1-\nu_L}{1+\nu_L}. \quad (3)$$

We consider again a Fabry-Perot structure as depicted in Fig. 2, where the distance between the reflective surfaces of the measurement channel can be written as a function of the same quantity for the reference channel, i.e. $D_{FP_M} = D_{FP_R} - 2d_L$. The wavelengths shifts $\Delta\lambda$ on each channel is therefore given by this relation (as we explained in [7]):

$$\left(\frac{\Delta\lambda}{\lambda}\right)_{R,M} = \left(\frac{\Delta D_{FP}}{D_{FP}}\right)_{R,M} + \left(\frac{\Delta n_{FP}}{n_{FP}}\right)_{R,M}. \quad (4)$$

As the refractive index variation of air Δn_{FP} is identical for the reference and measurement channels, we can write:

$$\Delta t_L = t_L \left(\frac{\Delta\lambda}{\lambda}\right)_R + \frac{D_{FP_M}}{2} \left(\left(\frac{\Delta\lambda}{\lambda}\right)_R - \left(\frac{\Delta\lambda}{\lambda}\right)_M \right) - t_L \frac{\Delta n_{FP}}{n_{FP}}. \quad (5)$$

As a result, we notice that this method requires evaluating precisely the relative refractive index variation of air Δn_{FP} , composing the cavity. This precise evaluation is required to determine the thickness variation with high accuracy. In this matter, we employ the Ciddor equation [8-10], detailed in [11], that gives an accuracy on Δn_{FP} better than 10^{-6} , subject to know the surrounding pressure P (with 5 mb of accuracy) and temperature T (with 2°C of accuracy).

4. OPTICAL STUDY

We investigate simulation software to take into accounts all modifications caused by a thermal change on the properties of the various materials composing the interferometer. Therefore, the refractive index and thickness variations are simulated, as well as the wavelength dependence of the refractive index, to finally evaluate the wavelengths shifts we get on each channel. We aim to determine the coefficients α_L and ν_L for the layer. As we reported in Section 3, we have to consider several substrates with different CTE α_s . We selected 5 glass substrates with the following CTE: $3.10^{-8}/^\circ\text{C}$, $5.5.10^{-7}/^\circ\text{C}$, $71.10^{-7}/^\circ\text{C}$, $101.10^{-7}/^\circ\text{C}$ and $142.10^{-7}/^\circ\text{C}$. For the dielectric layer, we consider two common materials used in interference thin-film filters, i.e. silica (SiO_2) and tantala (Ta_2O_5). Their properties, described by the one of the bulk material for silica layer, and by [5] for tantala, are given in Table 1.

Dielectric material	α_L ($10^{-7}/^\circ\text{C}$)	ν_L	β_L ($10^{-7}/^\circ\text{C}$)	p_{11}	p_{12}
Silica SiO_2	5.5	0.17	69	0.121	-0.068
Tantala Ta_2O_5	24.2	0.23	23	0.270	0.163

Table 1: Properties of available dielectric materials in simulation software

Our method, estimating the thickness variation Δt_L , is based on accurate measurements of wavelengths. We study also the consequence of a noise on these measurements and on their associated shifts. We therefore chose to carry out a statistical approach and we report here the result obtained by considering an additive white Gaussian noise, with amplitude of 1 pm and 0.05 pm. Figures 6 and 7 compare the resulting thickness variations calculated through Eq. 5 with the corresponding noises. We simulate 300 measures for each CTE associated to each substrate, and we report the error bars calculated at 3σ , where σ is the standard deviation.

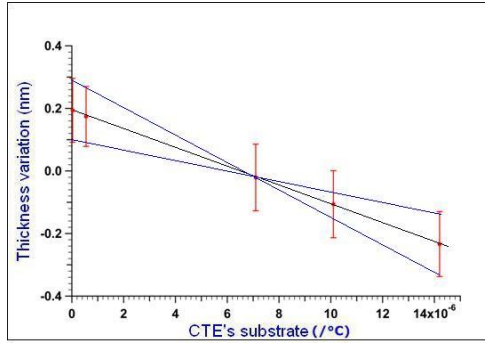


Figure 6: Thickness variation and associated error bars while considering a white Gaussian noise with amplitude of 1 pm. The different lines shows the extremes values taken by slope and value for $\alpha_s=0$.

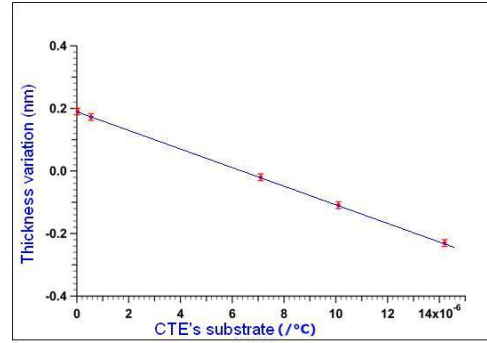


Figure 7: Thickness variation and associated error bars while considering a white Gaussian noise with amplitude of 0.05 pm.

Figures 6 and 7 illustrate the fact that the slope and the value for $\alpha_s=0$ depend on the precision reached on the determination of the wavelengths corresponding to the resonances of the Fabry-Perot structures and their shifts under the temperature change ΔT . Consequently, these α_L and ν_L values could be erroneous. We thus report in Table 2 the expected errors versus the wavelengths accuracy, for the two materials considered.

Material/wavelength accuracy	mean α_L ($10^{-7}/^\circ\text{C}$)	$\Delta\alpha$ at 3σ ($10^{-7}/^\circ\text{C}$)	mean ν_L	$\Delta\nu$ at 3σ
SiO ₂ / 1 pm	5.6	2.2	0.170	0.019
Ta ₂ O ₅ / 1 pm	24.1	2.2	0.230	0.015
SiO ₂ /0.05 pm	5.5	0.2	0.170	0.002
Ta ₂ O ₅ /0.05 pm	23.9	0.3	0.228	0.002

As a consequence, we need to consider an accuracy of about 0.05 pm on the determination of wavelengths resonances and associated shifts of the interferometer in order to reach a convenient accuracy on α_L and ν_L .

The second important point to consider is the parallelism of the two mirrors composing the interferometer, as the thickness variations we need to detect are typically a few tens of picometers. Hence, even a low default of parallelism may induce errors on the measurement of thickness variations for the dielectric layer, and consequently causes errors on the coefficients α_L and ν_L . In addition, through our simulation software, we demonstrate that it is necessary to consider several reference channels symmetrically disposed around the measurement channel, in order to enhance the tolerance on the parallelism. In Eq. 5, the wavelengths resonances and associated shifts for the reference channel are calculated as the average values obtained from every reference channel. As a compromise, we chose to consider three reference channels, disposed on a circle of 13 mm of diameter around the centre channel (measurement channel), that form also an equilateral triangle. We illustrate these different channels in Fig. 8.

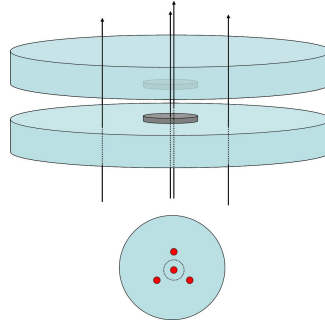


Figure 8: Scheme of the 4 channels. The 3 others composed the reference channels, and the centered one includes the dielectric layer to be studied. To enhance the tolerance on parallelism between the two mirrors, we consider the average measures carried out the reference channels.

Nevertheless, a default of parallelism between the two mirrors still causes a degradation of the interference fringes, because of the averaging effect on the diameter of the beam, and it is then difficult to extract the wavelengths resonances if this effect becomes too large. Hence, we simulate this degradation effect for the effective diameter defined for each channel, i.e. 2 mm. The parallelism should be better than 30 arc-seconds that is, in the experimental point of view, accessible.

Finally, as established by Eq. 1 and Eq. 2, a thermal change induces variations on thickness variations and on refractive index. Thus, when we measure the wavelength shifts in the measurement channel, a part is attributed to the refractive index variation of the dielectric layer which we neglect to express the quantity Δt_L by Eq. 5. As we mentioned before, the thermo-mechanical configuration is mainly sensitive to the thickness variation of the dielectric layer thanks to the deposit of silver coatings. To determine the minimal thickness of silver required to be insensitive to the refractive index variation, we simulate the absolute wavelengths shifts obtained in the measurement channel in two cases, as a function of the deposited silver thickness. For the first case, we take into account all the modifications due to the thermal change, and notably the refractive index of the dielectric layer given by Eq. 3. For the second case, we do not include the dependence of the refractive index of the dielectric layer with temperature. We compare then the absolute wavelengths shifts simulated versus the silver thickness, as illustrated by Fig. 9.

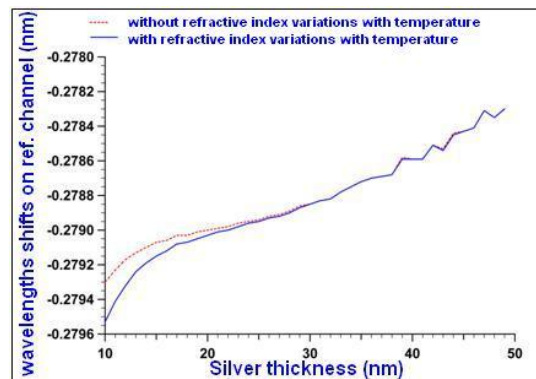


Figure 9: Comparison of the wavelengths shifts obtained on the measurement channel versus the silver thickness, while considering or not the refractive index dependence with temperature for the dielectric layer.

For a silver layer thick of around 40 nm, the two curves are identical, meaning that the Fabry-Perot interferometer is mainly sensitive to the thickness variation of the dielectric layer. The information contained in the wavelengths shifts is therefore not affected by the refractive index variations. This result is of a great importance to prove that this method can be used to evaluate the coefficient α_L and ν_L with efficiency.

By taking into account all parameters able to cause errors on the determination of the coefficients of the dielectric layer, the simulation proves that we can expect an accuracy of $0.7 \cdot 10^{-8}/^{\circ}\text{C}$ on the coefficient α_L , and $0,8 \cdot 10^{-2}$ on ν_L with this method. These precisions are for instance sufficient to predict with a high accuracy the behavior of DWDM filters under a thermal change.

5. MECHANICAL STUDY

As the CTE of materials composing the interferometer are not equal, a thermal change also causes deformations of the interferometer plates [12, 13]. It induces a problem of reference, and consequently errors on the extraction of the coefficients of the dielectric layer. To evaluate precisely this effect, we simulate the thermal behavior of the interferometer by a Finite Element Method (FEM). To reach precise results, we need to simulate a realistic configuration, close to the one experimentally implemented. We envisage to use the plates in a horizontal configuration to avoid a maintaining system for the control of the distance and the adjustment of the parallelism between mirrors. In addition, this configuration (especially when thermal changes are applied) is much easier to simulate than a vertical one. In such horizontal configuration, the mirrors will have different diameters, in order to put them on two adapted supporting tubes. One of them is provided with a system allowing the control of distance and parallelism between blades (better than 30 arc-seconds). Figure 10 depicts the structure we simulate by FEM. The thickness of the silver, the thickness of the dielectric layer, the thickness of the cavity and the thickness of the substrate are respectively 40 nm, 1 μm , 60 μm and 5 mm. The superior blade has a diameter of 30 mm, the inferior one 25 mm, and the dielectric layer is a disk of 4 mm. It is important to stress here that the large ratio between the thickness of the layers and the overall dimensions of the structure is difficult to simulate by FEM, especially in regard of the meshing operation.

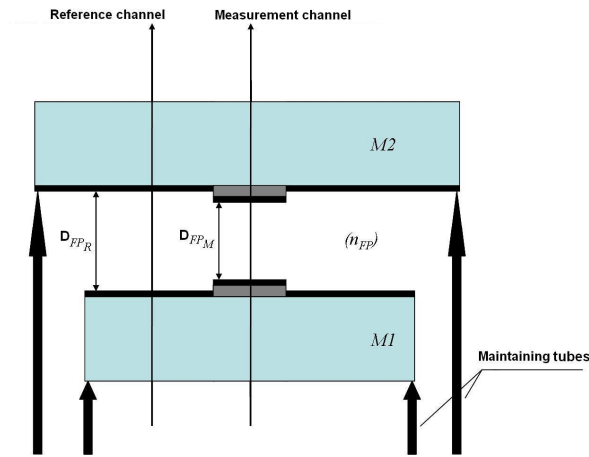


Figure 10: Horizontal configuration of the Fabry-Perot interferometer simulated by FEM, and dedicated to the extraction of the coefficients of α_L and ν_L of the dielectric layer.

Our simulation by FEM allows us to evaluate, after the temperature change, the thickness cavity as a function of the radial coordinate r . We consider that the value measured by our channel corresponds to the average value of the thickness cavity on the diameter of laser beam (i.e. 2 mm). We remark that a classical calculation of thermal strain by the Stoney formulae [14] cannot be carried out here, since we do not have a coating on the whole surface of substrate. As we notice by the FEM, while comparing a circular disk shape with a 4 mm of diameter deposited on a substrate (25 mm of substrate) and a coating all over the substrate, the induced deformations are not the same for the two studied cases. At last, we consider for all our simulations a thermal change $\Delta T=50^\circ\text{C}$.

Without thermal strains between materials (i.e. in the case where all the CTE are identical), the comparison between the thickness cavity of reference and measurement channel gives exactly the thickness variation for the dielectric layer we

expect by the relation $\Delta t_L = \frac{1}{2} (\Delta D_{FP_R} - \Delta D_{FP_M})$. When the CTE of the materials are different (realistic case), the

structure gets out of shape. We aim to minimize this thermal strain due to the dielectric layer and the silver coatings, the following subsections report and describe the means we utilized to reach this objective. We recall that our goal is to precisely evaluate the thickness variation of the dielectric layer versus the substrate CTE, in order to access to the coefficients α_L and ν_L .

5.1. Minimization of thermal strain caused by the dielectric layer

To minimize this strain, we propose to consider a symmetric deposit for the dielectric layer, meaning on each blade composing the interferometer. It is a standard and quite spontaneous way to compensate the thermal stress induced by

the thermal change. We simulate also a Fabry-Perot interferometer without silver coatings, to dissociate the influence of the different contributions implying errors on the extraction of the thickness variation of the dielectric layer. The new configuration is depicted in Fig. 11. For clarity, we introduce composite variables ξ and ε defined by

$$\xi = (\alpha_s - \alpha_L) \frac{Y_L}{1 - \nu_L} \frac{1 - \nu_s}{Y_s} \quad \text{and} \quad \varepsilon = (\Delta t_L)_{FEM} - (\Delta t_L)_{expected}.$$

In these relations, the index S and L report respectively to the substrate and to the layer, and the quantity Y designed the Young's modulus of the materials. The variable ξ contains all parameters involved in the thermal strain, apart from the thickness of materials, and the variables ε is the measured error on thickness variation caused by the strain effect. We are then interested in the curve $\varepsilon=f(\xi)$.

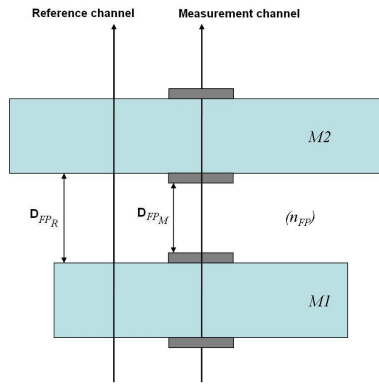


Figure 11: First study of the thermal strain caused by the dielectric layer. The structure considered has no silver coatings.

Simulations show that these functions strongly depend on the substrate thickness, as it is illustrated in Fig. 12, for a tantala layer with different thicknesses.

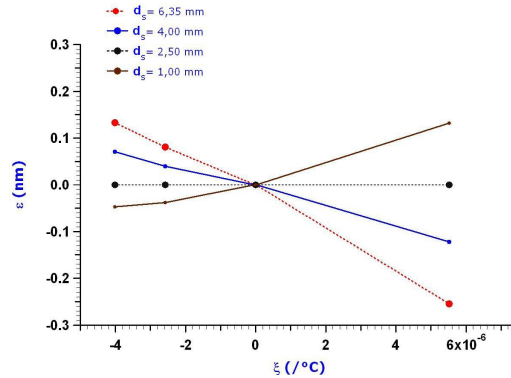


Figure 12: Errors caused by the thermal strain on the thickness variation of the dielectric layer (here tantala)

We remark, for each curve, that for the abscise $\xi=0$, the errors vanishe. This point corresponds to the case where the coefficients $\alpha_s=\alpha_L$, and therefore there is no strain induced by the temperature change. Moreover, a surprising result is that the substrate possesses an optimal thickness, for which the errors are minimal and this for all considered substrates with different CTE. We varied all parameters linked to the interferometer, and after that we can conclude that the optimal thickness of the substrate depends only on the diameter of the dielectric layer deposited at the centre of blades, and that in through a linear relationship. We depict, in Fig. 13, the optimal substrate thickness we determined versus the dielectric diameter deposited at the centre. The relationship is perfectly linear, and for the diameter envisaged (4 mm), we determine an optimal substrate thickness of 2.8 mm.

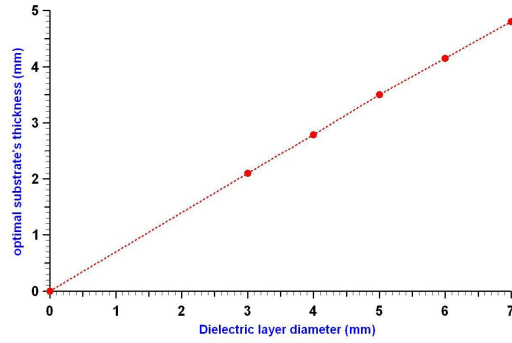


Figure 13: Evolution of the optimal substrate thickness versus the dielectric diameter deposited at the centre of the interferometer.

5.2. Thermal strain caused by silver coatings

If we consider now silver coatings, we observe that the thermal strains are too important to obtain a good accuracy on the evaluation of the thickness variation Δt_L . We cannot use symmetric deposits, since the reflectance of the mirrors is around 90%, and thus the light passing through the interferometer would be too attenuated. The method we envisage is to consider partial deposit to minimize the area of the metallic surfaces, and accordingly their impact. Therefore, we consider a metallic disk of 3 mm of diameter above the dielectric, and a 3 mm wide ring for the reference channel. This is illustrated in Fig. 14. Nevertheless, despite this design change, the strains are still too large to evaluate precisely the thickness variation. Hence, we decide to investigate the possibility that the strains, caused by silver coatings, are additive. If this hypothesis is true, then the strains can be subtracted by studying the thermal behavior of a reference structure as represented by Fig. 15. Following this hypothesis, the method for the extraction of the thickness variation of the dielectric layer is carried out in two steps. First, we evaluate the quantity ρ_{metal} defined by $\rho_{metal} = (\Delta D_{FP_R} - \Delta D_{FP_M})_{t_L=0}$, considering a thermal change on our reference structure (Fig. 15). Second, we introduce this quantity in the evaluation of the dielectric thickness variation while considering a thermal change in our measured structure (Fig. 14). The dielectric thickness variation Δt_L is also determined by:

$$\Delta t_L = \frac{1}{2} (\Delta D_{FP_R} - \Delta D_{FP_M} - \rho_{metal}) \quad (6)$$

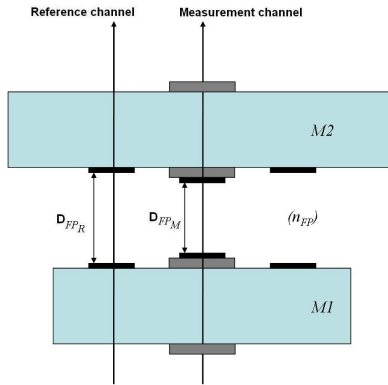


Figure 14: Measured structure with partial silver coatings, dedicated to the determination of dielectric thickness variation.

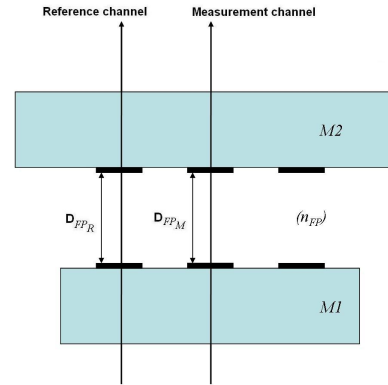


Figure 15: Reference structure dedicated to the measurements of strains induced by silver coatings

Figures 16 and 17 illustrate the results $\varepsilon=f(\xi)$ obtained without introducing the corrective term ρ_{metal} (Fig. 16) and with it (Fig. 17), to evaluate the dielectric thickness variation. By taking into account the corrective term ρ_{metal} , we obtain the same straight than we had in the subsection 5.1, i.e. in considering the thermal change on an interferometer without silver

coating. We also find again the same optimal substrate thickness, and the dielectric thickness variation can be determined by this way with a good accuracy (and consequently, the coefficients α_L and ν_L).

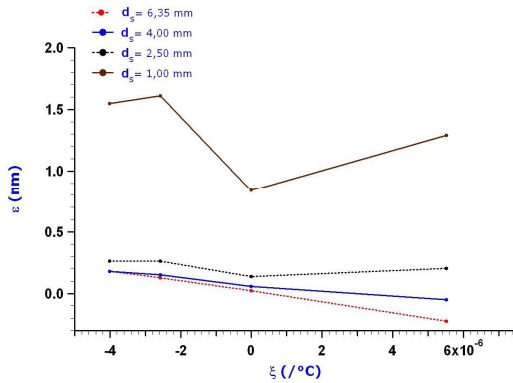


Figure 16: Errors ε caused by the strain defect without considering the introduction of the corrective term ρ_{metal} .

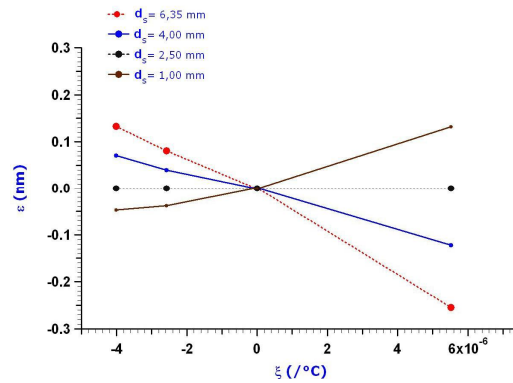


Figure 17: Effect of the introduction of the corrective terms ρ_{metal} on the relation $\varepsilon=f(\xi)$. This graph is to be compared with the Figure 16, where the corrective term is not used. Here, we have the same results than if we study the thermal behavior of the interferometer without silver coatings.

Finally, if we consider a Fabry-Perot structure with a substrate thickness of 2.8 mm, and if we determine the straight $\Delta t_L=f(\alpha_s)$, we can evaluate the coefficient α_L (by considering the value of this straight for $\alpha_s=0$) with an accuracy of $5.10^{-8}/^\circ\text{C}$, and the coefficient ν_L (by the slope of the same straight) with an accuracy of 5.10^{-4} .

6. CONCLUSION

We described in this paper a new optical method to determine with high accuracy the coefficients α_L and ν_L for a dielectric layer deposited at the centre of an interferometer. We remark that this method does not depend on the properties of the layer, and therefore it can be apply to every dielectric material we need to characterize. It is useful to predict with exactitude the behavior of an optical component using dielectric materials (like DWDM telecommunications filters which need to have a well-performed thermal stability). This method is based on the determination of the dielectric thickness variation under a thermal change versus the substrate CTE α_s , in this matter we only need to evaluate the slope and the value for $\alpha_s=0$ of the linear relationship. Since we want to detect small variations (typically a few tens of picometers), we use Fabry-Perot interferometer to enhance the sensitivity of measurement.

From an optical point of view, the method requires the determination of spectral resonances with 0.05 pm accuracy. Moreover, we need to dispose of several reference channels to enhance the tolerance on parallelism between the mirrors. From a mechanical point of view, a thermal change also causes strains on interferometer blades. We developed a dedicated Finite Elements Modeling to evaluate the errors caused by this deformation. We showed that to be efficient, it is necessary to study two quasi identical interferometers: the first without dielectric but with silver and the second with dielectric and silver. This way strains caused by silver coatings can be evaluated and eliminated. We conclude by the existence of an optimal substrate thickness (2.8 mm in our case), in order to reach a good accuracy on the determination of the dielectric thickness variation, and consequently the coefficients α_L and ν_L . It means that, for each point of the straight $\Delta t_L=f(\alpha_s)$, two Fabry-Perot structures are mandatory, and consequently the method requires at least 4 Fabry-Perot structures composed by 2 different substrates (with 2 different α_s , two points being obviously required to draw the straight).

This method is experimentally feasible, and a dedicated set-up integrating all the reported specifications should be developed, in order to properly evaluate these coefficients. Moreover, the same approach must be followed to estimate the TCRI and the elasto-optical coefficients p_{11} and p_{12} , by considering this time the behavior of the thermo-optical configuration we mentioned at the beginning.

REFERENCES

- [1] H. Takashashi, "Temperature stability of thin-film narrow-bandpass filters produced by ion-assisted deposition," *Appl. Opt.* **34**, 667- (1995)
- [2] R. Parmentier and M. Lequime, "Substrate-strain-induced tunability of dense wavelength-division multiplexing thin-film filters," *Opt. Lett.* **28**, 728-730 (2003)
- [3] M. Lequime, "Tunable thin-film filters: review and perspectives," in *Advances in Optical Thin Films*, Claude Amra, Norbert Kaiser, H. Angus Macleod eds., *Proc. SPIE* **5250**, 302-311 (2003)
- [4] N. Inci, "Simultaneous measurements of the thermal optical and linear thermal expansion coefficients of a thin film etalon from the reflection spectra of a super-luminescent diode," *J. Phys. D: Appl. Phys.* **37**, 22, 3151-3154 (2004)
- [5] D. Coyne, "Beamsplitter coating strain induced radius of curvature," Advanced LIGO, 2005
- [6] O Hiroyuk, "Change of mechanical properties of Ta2O5 thin film, Japan Society of mechanical engineers," 2000
- [7] S. Michel, "Ultrafine measurement of the thermal shift of Fabry-Perot resonances," *Proceedings of SPIE*, (**7102**) (2008).
- [8] P.E. Ciddor, "Refractive index of air: new equations for the visible and near infrared," *Applied Optics.* **35**, 1566-1573 (1996)
- [9] P.E. Ciddor, "Refractive index of Air: the roles of CO2, H2O, and refractivity virials," *Applied Optics*, **41**(12), 2292-2298 (2002)
- [10] E. Edlen, "The refractive index of Air," *Metrologia*, 2(2), 71-80 (1966)
- [11] J.A. Stone and J.H. Zimmerman. "Index of Refraction of Air," calculation and details available on: <http://emtoolbox.nist.gov/Wavelength/Documentation.asp> (2002).
- [12] R. Thielsch, A. Gatto, and N. Kaiser, "Mechanical stress and thermal-elastic properties of oxide coatings for use in the deep-ultraviolet spectral region," *Applied Optics.* **41**(16), 3211-3217, (2002).
- [13] S. Tamulevicius, "Stress and strain in the vacuum deposited thin films," *Vacuum.* **51**(2), 127-139 (1998).
- [14] G.G. Stoney, *Proceedings of Royal Society Of London.* **82**, 172 (1909).